ISSN: 2277-9655
Impact Factor: 4.116
CODEN: IJESS7

IJESRT

INTERNATIONAL JOURNAL OF ENGINEERING SCIENCES & RESEARCH TECHNOLOGY

CONTROL OF HYDROGEN ASSISTED CRACKING IN HIGH STRENGTH STEEL WELDS

Vinay Kumar Pal*, Dr. L. P. Singh, C.Pandey

* M. Tech, SHUATS, ALLAHABAD Department of Mechanical Engineering Sam Higginbottom University of Agriculture, Technology And Sciences (U.P State Act No. 35of 2016, as passed by the Uttar Pradesh Legislature) Allahabad, India

Assistant Professor, SHUATS, ALLAHABAD Department of Mechanical Engineering Sam Higginbottom University of Agriculture, Technology And Sciences (U.P State Act No. 35of 2016, as passed by the Uttar Pradesh Legislature) Allahabad, India

DOI: 10.5281/zenodo.557140

ABSTRACT

In present research work, the modified Granjon implant test was performed to evaluate the susceptibility of AISI 8620 and AISI 304 steel towards the hydrogen assisted cracking (HAC). Glycerine methods was employed to measure the diffusible hydrogen level (HD) in deposited metal for both the steels. The weld bead was deposited by using the Shielded metal arc welding (SMAW) process with basic type electrodes. The hydrogen was intentionally introduced for the plate of the material AISI 304 by using an oil of grade SAE 10, which is of very low viscosity. The fractured and un-fractured implant assembly were examined by using the field-emission scanning electron microscope (FESEM). The heat affected zone (HAZ) susceptibility is quantified by finding the lower critical stress (LCS) for a measured hydrogen content. The exact location of the fractures varied according to the type of materials being tested.

KEYWORDS: Hydrogen; HAC; LCS; CGHAZ; SMAW; Fracture.

INTRODUCTION

Hydrogen in the weldments is still continues to be seriously limiting the performance of the compounds. A number of intense research studies has have reported about the behaviour and effects of hydrogen in the steel and their welds [1–5]. It is proven that a sufficient amount of hydrogen if present along with the susceptible microstructure and the weld residual stress, poses a greater risk of hydrogen assisted cracking (HAC). It is very difficult to detect the HAC in the weldments due to the fact that it occurs at the ambient temperature and also, it appears hours or days after the completion of the welding. Therefore, even while in service it may cause the catastrophic failure of the components [6,7]. Hydrogen embrittlement (HE) is used as the index of HAC in the weldments. Basically, HE is a loss of mechanical properties caused due to the presence of hydrogen in atomic form and stress. The hydrogen gas enters the arc atmosphere and hence, it also enters the solidifying weld region in arc welding process. The risk of HAC depends on the crack susceptible microstructures, residual stress and the hydrogen content (H_D) in the deposited metals. The HAC is more significant in the ambient temperatures zone i.e. -50°C to 150°C. It is often of delayed nature i.e. cracks can appear even after several days of the completion of the welding as it is difficult to predict the HE. Usually, the hydrogen cracks are present either in HAZ or in weld metal itself, but it is very difficult to predict the crack propagation behaviour. It is widely accepted that for HAC to take place, the hydrogen content in the weld joint should be present along with the crack susceptible microstructure and tensile residual stress, as shown in **Fig. 1**.

ISSN: 2277-9655
Impact Factor: 4.116
CODEN: IJESS7

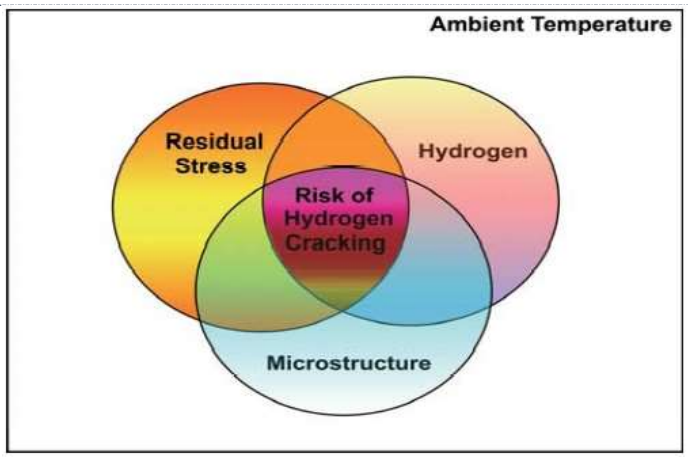

Fig. 1 Three essential conditions to cause HAC[8]

For the low alloy steels the risk of HAC increases with the increasing hardness of the microstructure. The microstructures developed in the weldments depends on the composition and the hardenability of the weld metal and the parent metal, the cooling rate and the prior austenitic microstructure before transformation. Carbon equivalent (CE) best describes the hardenability of the material. Higher the value of CE, higher will be the hardenability which indicates higher tendency to form cracks. The HAZ closest to the fusion zone (coarse-grained heat affected zone) transform to austenite as this region experiences the peak temperatures, and this austenitic microstructure can get transformed to hard martensite or bainite due to rapid cooling after welding. It is to be noted that due to the sufficiently high temperature coarse grain HAZ (CGHAZ) is formed which is more hardenable and less ductile than the regions further away from the fusion zone and hence, there is a greater risk of cracking in CGHAZ.

To determine the diffusible hydrogen content in the steel weldments, various methods has been developed and successfully employed by the researchers [9–12]. The most commonly used methods are: Glycerine Method, Mercury Method, Gas Chromatograph Method, and Hot Extraction Method. To estimate the hydrogen embrittlement susceptibility, the common used method are: Implant tests, Lehigh Restraint Test, RPI Augmented Strain Cracking Test, Controlled thermal severity (CTS) test and Lehigh Slot Weldability test [2,13]. In present days, implant tests is most commonly used method to estimate the hydrogen embrittlement susceptibility. The implant test, which was introduced by Henri Granjon at the Institute de Soudure (French Welding Institute) is an externally loaded test used to determine the susceptibility of HAZ towards hydrogen assisted-cracking. During implant test, a notched cylindrical specimen is prepared and inserted in the base plate of similar material, as shown in **Fig. 2**. A weld bead is deposited over the specimen such that the top portion lie in the fusion zone and the notch lie in the HAZ. After the completion of welding and before it becomes cold, a constant load is applied. The time to failure is recorded and a plot is obtained for stress applied versus the time to failure. The threshold stress level is hence determined which is called as lower critical stress (LCS).

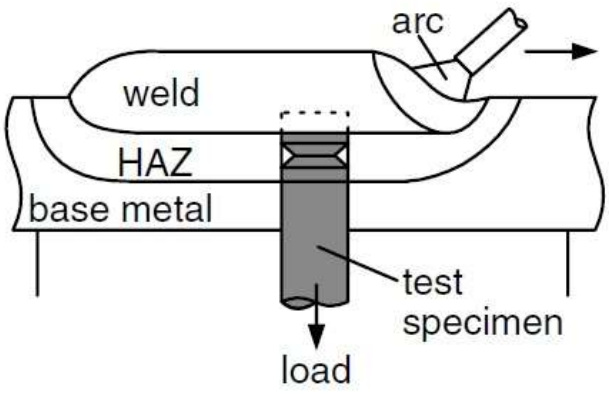

Fig. 2 Schematic of implant test

ISSN: 2277-9655
Impact Factor: 4.116
CODEN: IJESS7

Hydrogen in the weldments of high strength steels continues to seriously limit the performance of the components and confounds the quantitative component prognosis. Hydrogen is a transient element due to which it is difficult to measure the exact hydrogen content in the steel. At a given temperature, the residual hydrogen remain trapped and plays no role in HAC while the diffusible hydrogen is able to diffuse within or out of the weldment causes HAC. It is therefore more study is required for the determination of the diffusible hydrogen content and the fractography study is also required for the precise estimation of the behaviour of steel weldments under loading.

In present research work, the glycerin method is used for the diffusible hydrogen measurement in deposited metal on high strength AISI 8620 and AISI 304 steel. Fabrication of implant testing set-up was done to quantify the susceptibility of HAZ to HAC. The implant fracture specimen was also analysed to reveal the mode of fracture by using the FE-SEM.

MATERIALS AND EXPERIMENTAL DETAILS

Material and welding process parameters

High strength AISI 8620 and AISI 304 steel plate were used for the experiment. The chemical composition of materials are given in Table 1. The mechanical properties of virgin steel are depicted in Table 2. The weld bead was deposited by using the shielded metal arc welding process (SMAW). For both the material basic electrode was used. The welding process parameters and electrode designation are given in Table 3.

Table 1 Chemical composition of AISI 8620 and AISI304, wt%

Material	**Element, wt%**									
AISI 8620	**C**	**Si**	**Mn**	**P**	**S**	**Cr**	**Ni**	**Fe**	**Mo**	N
	0.15	0.38	0.81	0.009	0.02	0.53	0.83	96.77	0.26	-
AISI304	0.07	0.49	1.62	0.008	0.026	17.74	9.77	70.11	-	<0.005

Table 2 Mechanical properties of AISI 8620 and AISI304

Mechanical properties	AISI 8620	AISI304
Tensile strength (MPa)	559	620
Yield strength (MPa)	394	288
Young's modulus (GPa)	192	196
Vicker's hardness (HV)	211	127

Table 3 Welding procedure and parameters used for AISI 8620 and AISI304

Welding conditions	AISI 8620	AISI304
Welding process	SMAW	SMAW
Electrode type	Basic electrode of AWS Code : E7018-1	Basic electrode of AWS Code : E308-16
Electrode diameter	4 mm	4 mm
Electrode reconditioning	Preheat at 100 °C for 4 hours	Preheat at 100°C for 4 hours and then dipped in oil (SAE 10 grade) for 30 min.
Voltage	25 V	25 V
Current	160 A	140 A
Travel speed	2.5 mm per sec	2.5 mm per sec

Implant tests

Implant testing allows evaluation of a material's true heat-affected zone susceptibility to hydrogen induced cracking. The implant tests was performed as per AWS standards (i.e. B4.0-98) and IIW guidelines. Test block specimen, a small cylindrical specimen (implant specimen) is machined with a helical notch at one end and fit into a hole drilled in a base metal specimen plate as per **Table 4**.

ISSN: 2277-9655
Impact Factor: 4.116
CODEN: IJESS7

Table 4 Dimensions of base plate and implant specimen

Base plate	
Plate thickness	9.52 mm
Plate width	50.80 mm
Plate length	66.68 mm
Hole diameter at the centre	6.35 mm
Implant specimen	
Total length (except gripping length)	41.27 mm
Gripping diameter	9.52 mm
Thread type	¼ - 28 UNF
Pitch	0.907 mm
Major diameter	6.35 mm
Minor diameter	5.24 mm
Thread length	9.52 mm
Thread angle	60 degrees
Thread root radius	0.1 Mm

As per pre-specified welding parameters a weld bead was deposited on the top surface of the specimen plate directly over the threaded sample and hole, as shown in **Fig. 3**. The implant assembly was allowed to cool for 2 minutes at room temperature. After the cooling, the entire implant assembly was quenched in an alcohol ice bath at 0°C until loading. Within 10 minutes after quenching the implant assembly was placed in the Universal Tensile testing Machine (Instron 5982) and the desired test load is applied. After fracture of the specimen the load and time to rupture was recorded. The experiment was repeated for number of specimens with different stress levels. The maximum stress level sustained for a period of 24 hours was considered as lower critical stress (LCS). The LCS is the threshold level of stress at which diffusible hydrogen even if present in sufficient amount for the crack propagation it will not propagate.

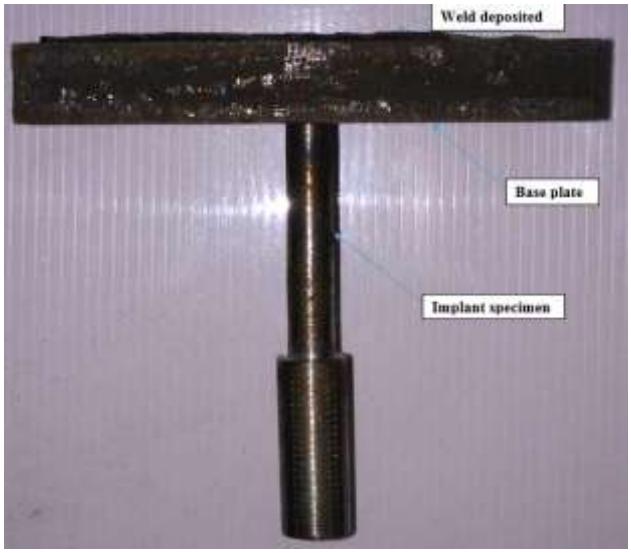

Fig. 3 Implant test assembly

Diffusible hydrogen measurement

Glycerine test was used for measuring the mounts of diffusible hydrogen content present in the deposited metal as per Indian standards IS 11802 (1986). Hydrogen specimens were prepared of 125 mm × 25 mm× 12 mm. Glycerine test setup was turned on 4-5 hours prior to the actual test, as glycerine was to be maintained at 45°C which require 4-5 hours for initial test. Single weld bead was deposited on 25 mm surface of 100 mm in length with same welding parameters as used in depositing bead on the implant assembly. Immediately after the bead deposition specimen were quenched in water at 20 °C for 30 s. After quenching specimen was stored in dry ice or liquid nitrogen until measurement. After that, specimen was introduced in an apparatus containing glycerine which

ISSN: 2277-9655
Impact Factor: 4.116
CODEN: IJESS7

was maintained at 45 °C. Hydrogen was collected from the deposited metal for 48 hours. The glycerine set-up is shown in **Fig. 4(a).** The test specimen is shown in **Fig. 4(b).**

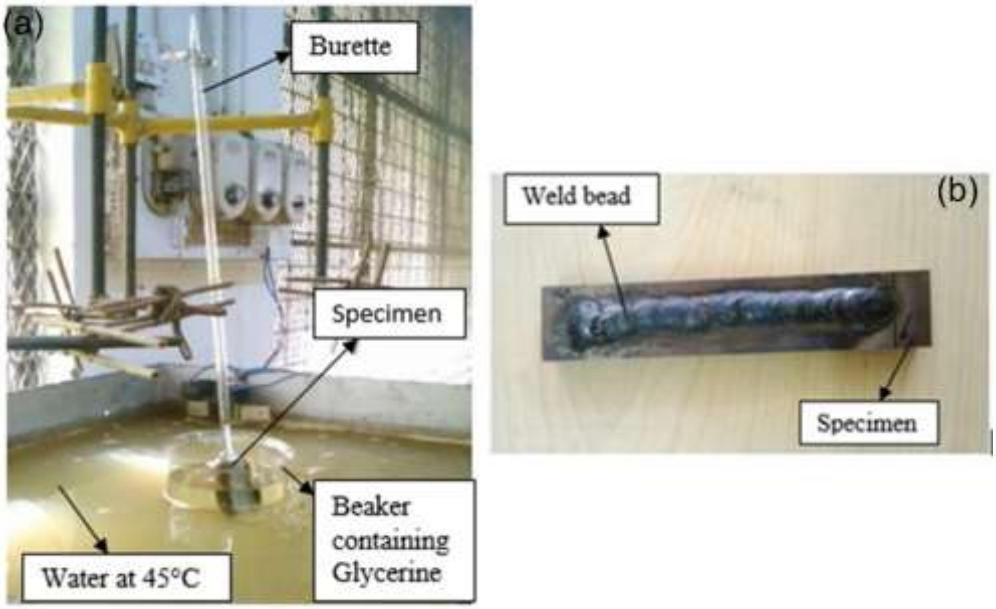

Fig. 4 (a) Glycerine test setup, (b) Glycerine test specimen

The average estimated (H_D) was estimated by using the following relation;

$$H_{Glycerine} = V_t\left(\frac{273}{273+T}\right)\left(\frac{P}{760}\right)\left(\frac{100}{W_f - W_i}\right)\frac{ml}{100g} \quad (1)$$

where, $H_{Glycerine}$ is diffusible hydrogen measured, V_t is volume of hydrogen measured at temperature T and pressure P, W_i is weight of specimen before welding and W_f is weight of specimen after removal from the glycerine apparatus.

Microstructure characterization and hardness measurement

The unfractured implant specimen was sectioned with help of wire EDM perpendicular to the welding direction through the axis of the implant specimens. The sample was grinded and polished by using the SiC emery paper upto grit size of 2000. After the paper polishing, the sample was etched in 5 % Nital solution for 60 s. the microstructure characterization was carried out by using the field-emission scanning electron microscope and optical microscope.

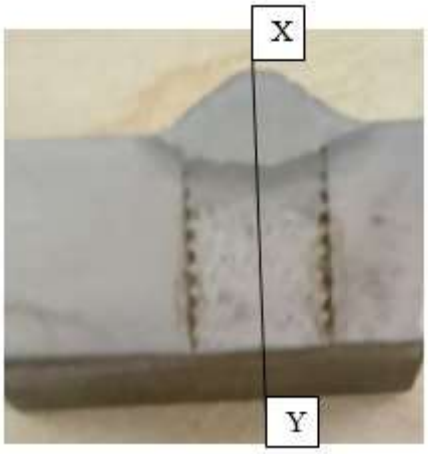

Fig. 5 Typical implant test specimen sectioned near the implant axis for AISI 8620, 5% nital etch

ISSN: 2277-9655
Impact Factor: 4.116
CODEN: IJESS7

Microhardness was recorded along the XY axis (implant axis) of unfractured sample, as shown in **Fig. 5**. The microhardness was recorded at load of 500 g with dwell time of 10 s. To examine the mode of fracture and relative amounts of each mode of fracture, the implant fracture surface was also examined by using the FESEM.

RESULTS AND DISCUSSION

Diffusible hydrogen content

The amount of diffusible hydrogen content was measured at T= 27 °C and P=760 mm for four specimens of AISI 8620 by Glycerine test and the average estimated ($H_{GLYCERIN}$) is corrected for STP which was calculated close to 4.62 ml per 100 g, whereas for the second case i.e. AISI 304, the average estimated ($H_{GLYCERIN}$) is corrected for STP which was calculated close to 9.48 ml per 100 g. This is due to the contamination of the electrodes with hydrocarbons for the 304 grade stainless steel. The increased level of hydrogen in AISI 304 was due to the pickup of oil in the electrodes while being dipped. It has been reviewed in recent research that the hydrogen embrittlement is more significant for the case where the H_D content is found to be more than 5 ml per 100g. Here, it can be observed with the AISI 304. The results of diffusible hydrogen measurement is depicted in **Table 5.**

Table 5 Diffusible hydrogen level content in deposited metal for AISI 304 and AISI 8620 steel

Weld type	Diffusible hydrogen content ($H_{Glycerine}$) (ml/100gm)			Mean diffusible hydrogen content ($H_{Glycerine}$) (ml/100gm)	Standard deviation for $H_{Glycerine}$ measurement
	Trial 1	Trial 2	Trial 3		
AISI 8620	4.58	4.65	4.62	4.62	0.035
AISI 304	9.4	9.45	9.60	9.48	0.104

Microhardness

The data obtained from Vickers hardness test is used to plot as shown in **Fig. 6(a-b)**. the microhardness reading are taken along the implant axis for both the steels, as shown in **Fig. 5.** Varation in hardness value across the deposited metal (weld fusion zone and HAZs) reveals the present of hetrogenious microstructure. For AISI 8620 steel, the hardness in weld fusion zone varied from 220-229 HV while, in AISI 304 varied from 233-265 HV. Maximum hardness value is noticed in CGHAZ for both the steels. The CGHAZ hardness was measured to be 298 HV and 301 HV for AISI 8620 and AISI 304, respectively. The CGHAZ hardness value are much higher than their respective BM hardness. That means the CGHAZ has a higher tensile strength than that of the base metal for the two steels. The higher strength and hardness of CGHAZ make it more susceptible for HAC. The hardness variation occurs due to the change of microstructures. The microstructures gets varied due to the different level and type of heat involved while and at the end of completion of welding. The lower hardness was measured in soft inter-critical heat affected zone (IC-HAZ), as shown in **Fig. 6**.

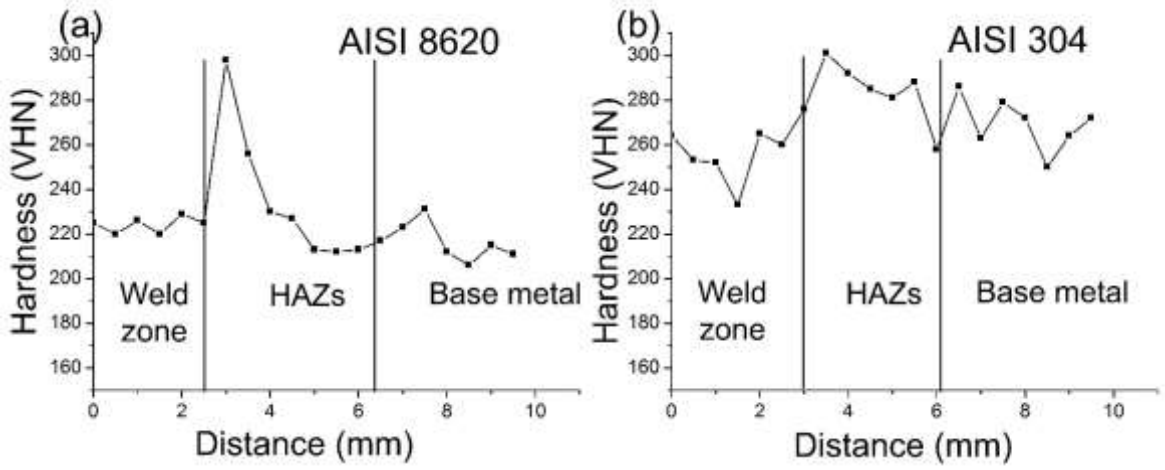

ISSN: 2277-9655
Impact Factor: 4.116
CODEN: IJESS7

Fig. 6 Vickers hardness versus the distance taken along the axis of the implant specimen; (a) For the material AISI 8620, and (b) For the material AISI 304

Lower critical stress

The data obtained from the implant testing is used to draw plot of applied stress versus time to rupture for each specimen, as shown in **Fig. 7(a-b)**.

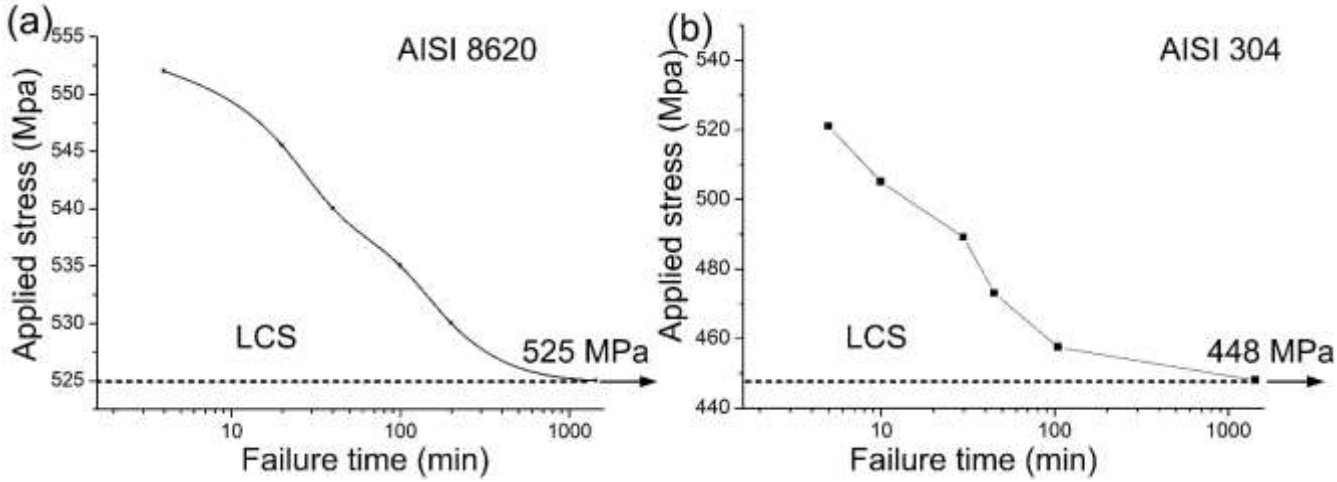

Fig. 7 Stress versus time to failure; (a) For the material AISI 8620, and (b) For the material AISI 304

The implant test results are depicted in **Table 6.** The **Table 6** consisted of following terms;

(a) The microhardness value of CGHAZ was converted to CGHAZ tensile strength by using the hardness conversion chart for both the steel.
(b) The embrittlement index of steels was represented as the ratio of LCS to tensile strength of CGHAZ.

Table 6 Implant test results

Experiment Case	Diffusible hydrogen content (ml/100 gm)	CGHAZ Max Hardness (HV)	CGHAZ tensile strength (MPa)	Lower critical stress (MPa)	Embrittlement index
AISI 8620	4.62	298	965	525	0.54
AISI 304	9.48	301	975	448	0.45

The embrittlement index (EI) of AISI 8620 is close to 0.54 whereas embrittlement index for AISI 304 was found close to 0.45. The decrease in the value of embrittlement index was the result of introduced H_D in the deposited metal of AISI 304. The electrode being contaminated with lubricating oil of grade SAE 10 resulted in the pickup of hydrogen in the welds of AISI 304. The electrode used for AISI 8620 was not contaminated with any kind of oil and hence, very less introduction of hydrocarbons. It is to be noted that lower value for the embrittlement index in particular material indicate increased susceptibility to hydrogen embrittlement. The EI mainly depend on the LCS value because the CGHAZ hardness does not show a significant variation. High EI value indicates the better performance of material in the weld condition. The CGHAZ strength after conversion was 965 MPa and 975 MPa for AISI 8620 and AISI 304 steel, respectively. Hence, result showed that AISI 8620 steel have less susceptibility to HAZ HAC compared to AISI 304 steel.

Metallographic examination

The optical micrographs were taken for study of microstructures from unfractured specimens near the LCS. Note that the HAZ in the implant specimen is much wider than that in the adjacent plate as shown in **Fig. 5**, due to the

ISSN: 2277-9655
Impact Factor: 4.116
CODEN: IJESS7

difference in heat flow and temperature gradient. Due to the excessive grain growth and possible formation of susceptible (high hardness) microstructure, HIC will most likely occur in the CGHAZ region, which is just adjacent to the fusion boundary. The optical micrograph of weld fusion zone and base metal is shown in **Fig. 8(a-d). Fig. 9 (a-d)** shows the SEM images for AISI 8620 and AISI 304, respectively. The EDS spectra of weld fusion zone and HAZ is shown in **Fig. 10(a-d).**

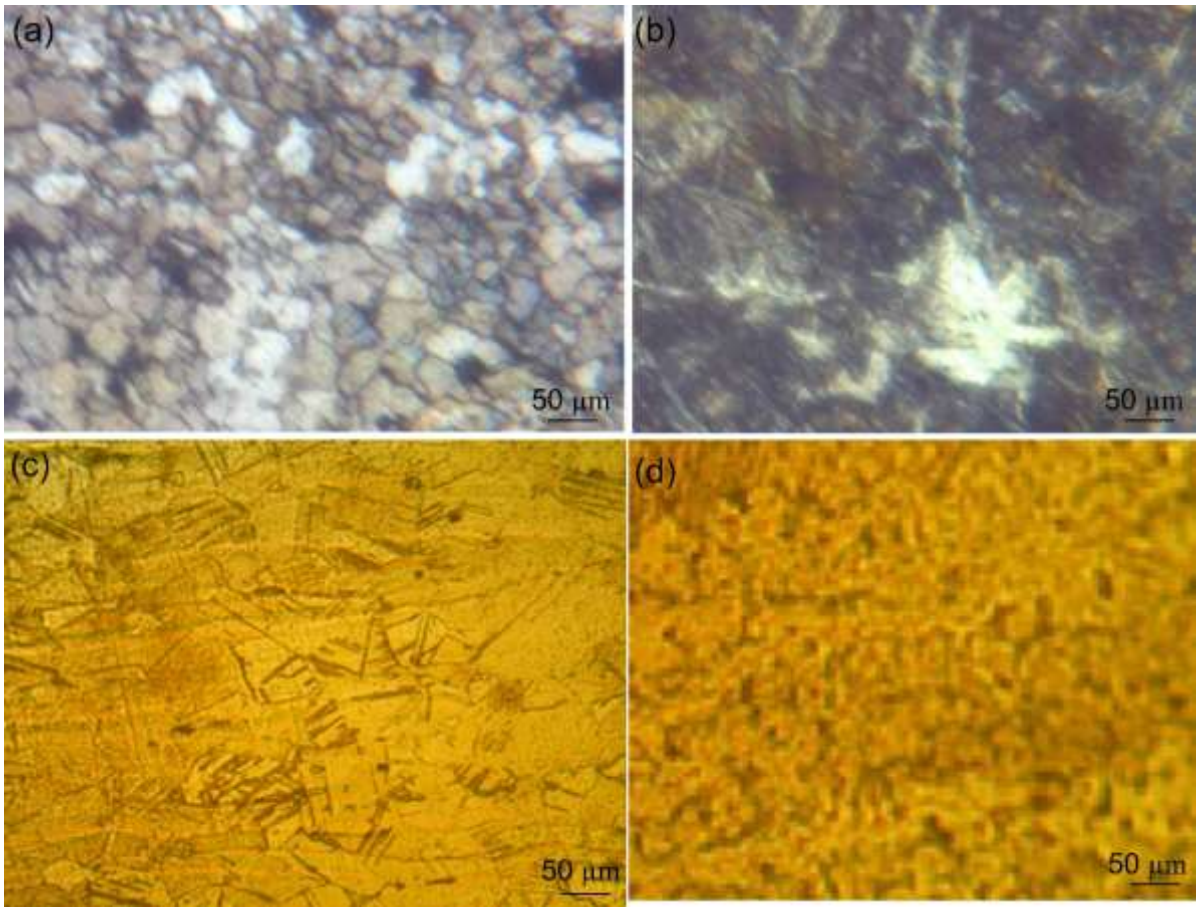

Fig. 8 Optical microscopy at 500x for unfractured specimen near LCS for AISI 8620; (a) BM, (b) WM; for AISI 304 (c) BM, (d) WM

ISSN: 2277-9655
Impact Factor: 4.116
CODEN: IJESS7

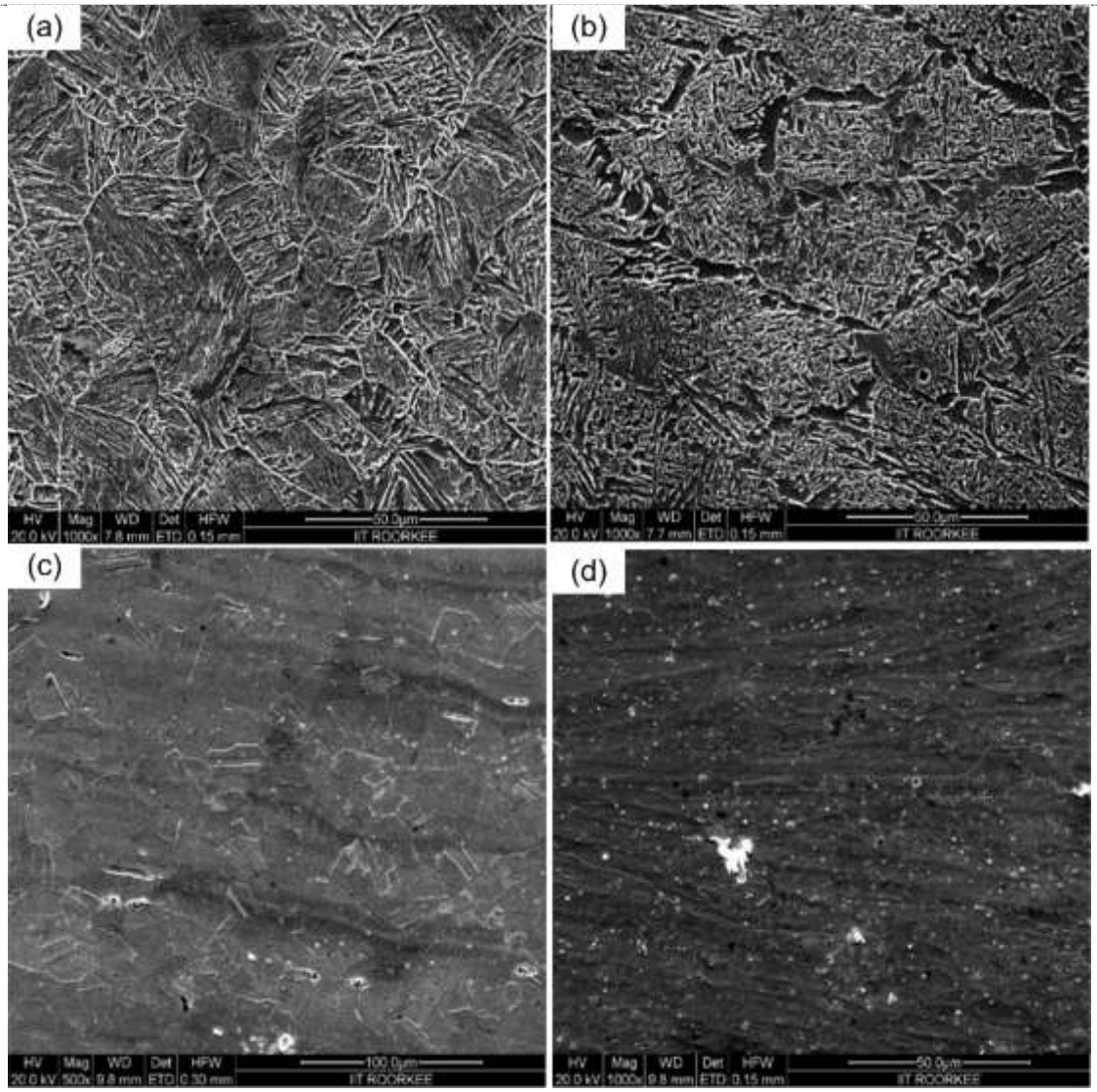

Fig. 9 Microstructures observed under SEM for unfractured specimen near LCS for AISI 8620 (a) BM, (b) WM; for AISI 304 (c) BM, (d) WM

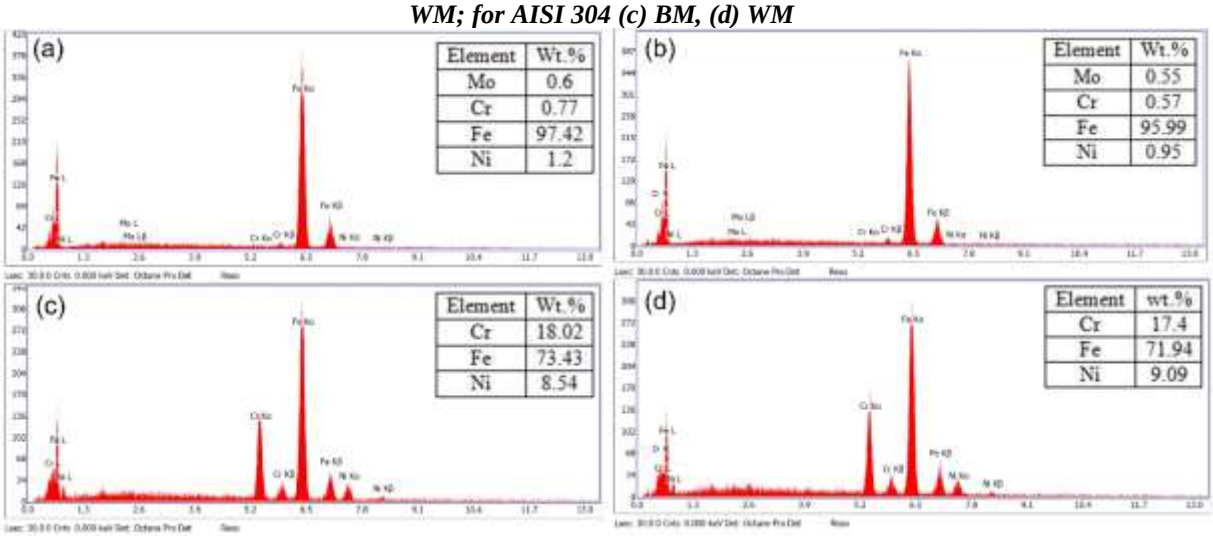

Fig. 10 EDAX for unfractured specimen near LCS for AISI 8620 for the region (a) weld zone, (b) HAZ; AISI 304 for region (c) weld zone, (d) HAZ

ISSN: 2277-9655
Impact Factor: 4.116
CODEN: IJESS7

Fracture surface morphology

Fig. 11 shows the fracture morphology of implant tested specimen of the material AISI 8620. It can be observed that final fracture occurred in mixed mode. The top view of fracture surface indicates the intergranular (IG) mode of fracture, as shown in **Fig. 11(a).** The cleavage facets are clearly seen in the crack initiation zone, as shown in **Fig. 11(b).** The presence of cleavage facet signifies the brittle mode of fracture in some regions. As the crack propagates, the quasi-cleavage (QC) mode of fracture is noticed, as shown in **Fig. 11(c).** In final fracture zone, the microvoid coalescence (MVC) is noticed, as shown in **Fig. 11(d-e).** The presence of dimples signifies the ductile mode of fracture. The region of dimples is more as compared with cleavage facet. Therefore, it can be concluded that the ductile mode of fracture is dominant and the fracture occurred in mixed mode i.e. ductile in some regions as well as brittle in some regions.

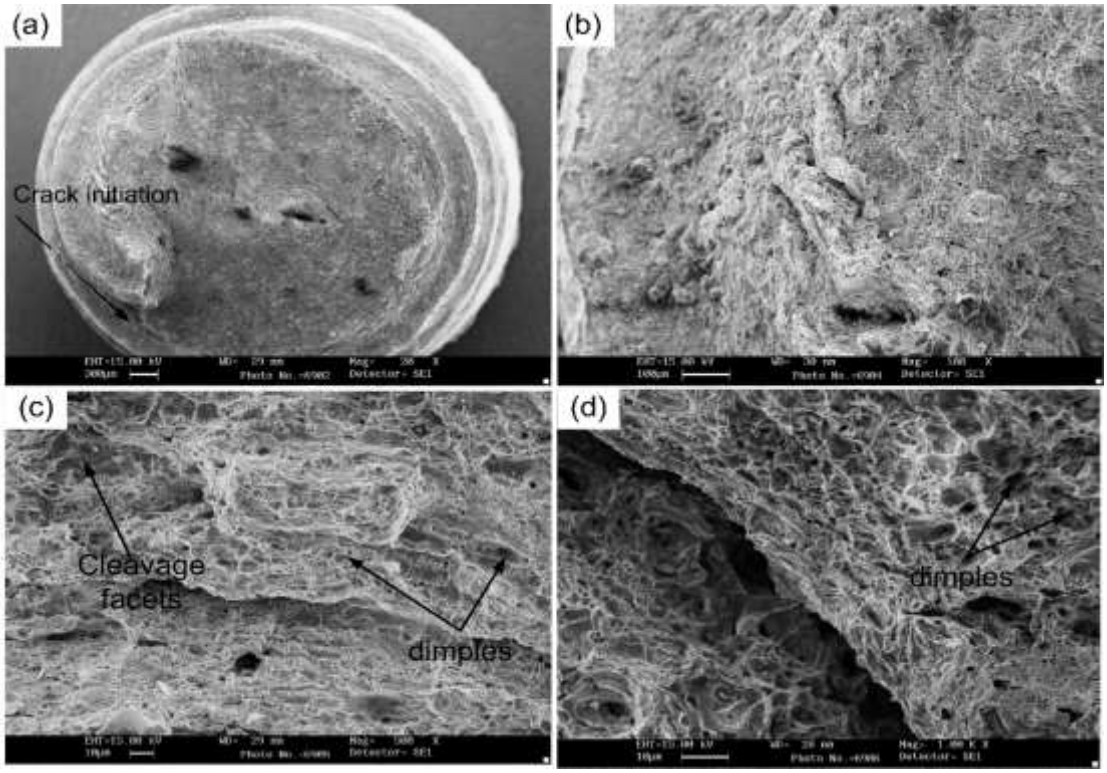

Fig. 11 Fracture morphology of AISI 8620 implant specimen; (a) Top-view of fracture surface, crack initiation zone (b) cleavage and dimples (c) final fracture zone (mixed mode), (d) microvoid coalescence

ISSN: 2277-9655
Impact Factor: 4.116
CODEN: IJESS7

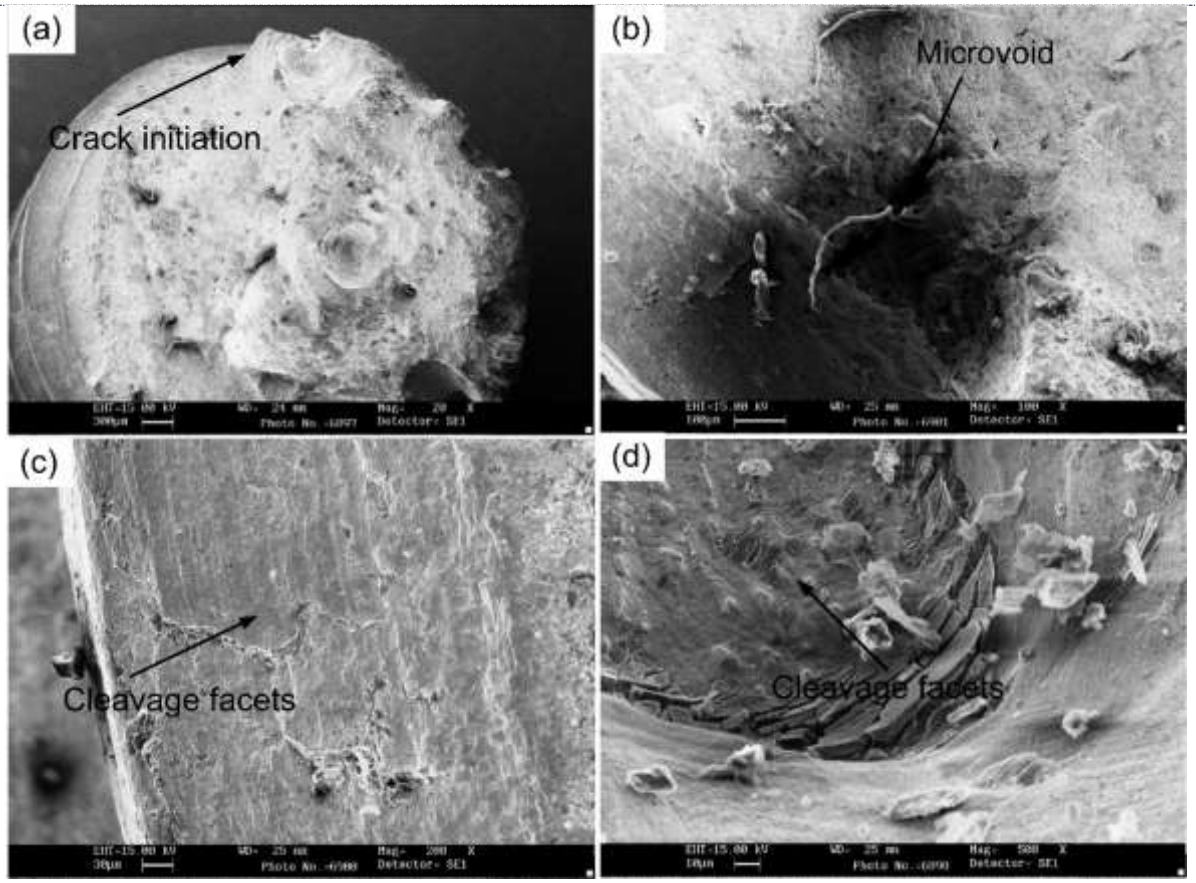

Fig. 12 Fracture morphology of AISI 304 implant specimen; (a) General fracture appearance of top view, (b) cleavage facets, (c), (d) Final fracture appearance

Fig. 12 shows the fracture morphology of the material AISI 304. The top view of fracture surface shows the large area of intergranular fracture (IG). It can be clearly observed that dimples is almost found to be absent in this case. The absence of dimples signifies the fracture has not occurred through ductile mode. The presence of cleavage facet is seen in almost all the regions. Therefore, it can be concluded that the mode of fracture is brittle mode. The cleavage facets are noticed both in crack propagation and final fracture zone, as shown in Fig. 12(b-e).

CONCLUSIONS

From the research work, the following conclusions has been made;

- For the given welding process parameters, the maximum Vickers hardness of CGHAZ is 298 HV and 301 HV for AISI 8620 and AISI 304, respectively. In CGHAZ, not a great variation in hardness was noticed for both the steel while in weld fusion zone the hardness varies from 220-229 HV for AISI 8620 and 233-265 HV for AISI 304 steel.
- The lower critical stress (LCS) was calculated to be 525 MPa and 448 MPa for AISI 8620 and AISI 304, respectively. The lower value of LCS indicates the higher susceptibility to HAC.
- Embrittlement index was calculated for AISI 8620 is close to 0.54 and for AISI 304 was found close to 0.45.
- The amount of diffusible hydrogen content was measured for four specimens of AISI 8620 by Glycerine test and the average estimated ($H_{GLYCERIN}$) is corrected for STP which was calculated close to 4.62 ml per 100 g, whereas for the second case i.e. AISI 304, the average estimated ($H_{GLYCERIN}$) is corrected for STP which was calculated close to 9.47 ml per 100 g.
- For AISI 8620 the ductile mode of fracture is dominant and the fracture occurred in mixed mode i.e. ductile in some regions as well as brittle in some regions. For AISI 304 the mode of fracture is brittle mode which can be concluded from the presence of cleavage facet and the absence of dimples.

ISSN: 2277-9655
Impact Factor: 4.116
CODEN: IJESS7

REFERENCES

[1] X. L. Feng and J. C. Lippold, 265 (n.d.).
[2] C. Pandey, N. Saini, M. M. Mahapatra, and P. Kumar, Int. J. Hydrogen Energy (2016).
[3] C. Pandey, M. M. Mahapatra, P. Kumar, and N. Saini, J. Eng. Mater. Technol. (2017).
[4] M. Glicerynową, 39, 47 (2013).
[5] G. Magudeeswaran, V. Balasubramanian, and G. Madhusudhan Reddy, Int. J. Hydrogen Energy 33, 1897 (2008).
[6] X. Yue, Weld. World 59, 77 (2014).
[7] A. W. Vasudevan, R. Stout, R. D. Pense, Weld. J. 60, 155 (1981).
[8] P. G. Kumar and K. Yu-ichi, Trans. JWRI 42, 39 (2013).
[9] D. Fydrych, A. ??wierczynska, and G. Rogalski, Metall. Ital. 107, 47 (2015).
[10] D. Fydrych and G. Rogalski, Weld. Int. 25, 166 (2011).
[11] D. Fydrych and J. Łabanowski, (2015).
[12] G. K. Padhy, V. Ramasubbu, and S. K. Albert, J. Test. Eval. 43, (2015).
[13] B. Y. W. P. Campbell, (n.d.).